

Reductive titration of photosystem I and differential extinction coefficient of P700⁺ at 810–950 nm in leaves

Vello Oja, Irina Bichele, Katja Hüve, Bahtijor Rasulov, Agu Laisk*

Tartu Ülikooli Molekulaar-ja Rakubioloogia Instituut, Riia tn. 23, Tartu, 51010, Estonia

Received 29 March 2004; accepted 11 June 2004

Available online 14 July 2004

Abstract

We describe a method of reductive titration of photosystem I (PSI) density in leaves by generating a known amount of electrons (e[−]) in photosystem II (PSII) and measuring the resulting change in optical signal as these electrons arrive at pre-oxidized PSI. The method complements a recently published method of oxidative titration of PSI donor side e[−] carriers P700, plastocyanin (PC) and cytochrome *f* by illuminating a darkened leaf with far-red light (FRL) [V. Oja, H. Eichelmann, R.B. Peterson, B. Rasulov, A. Laisk, Decyphering the 820 nm signal: redox state of donor side and quantum yield of photosystem I in leaves, *Photosynth. Res.* 78 (2003) 1–15], presenting a nondestructive way for the determination of PSI density in intact leaves. Experiments were carried out on leaves of birch (*Betula pendula* Roth) and several other species grown outdoors. Single-turnover flashes of different quantum dose were applied to leaves illuminated with FRL, and the FRL was shuttered off immediately after the flash. The number of e[−] generated in PSII by the flash was measured as four times O₂ evolution following the flash. Reduction of the pre-oxidized P700 and PC was followed as a change in leaf transmittance using a dual-wavelength detector ED P700DW (810 minus 950 nm, H. Walz, Effeltrich, Germany). The ED P700DW signal was deconvoluted into P700⁺ and PC⁺ components using the abovementioned oxidative titration method. The P700⁺ component was related to the absolute number of e[−] that reduced the P700⁺ to calculate the extinction coefficient. The effective differential extinction coefficient of P700⁺ at 810–950 nm was 0.40±0.06 (S.D.)% of transmittance change per μmol P700⁺ m^{−2} or 17.6±2.4 mM^{−1} cm^{−1}. The result shows that the scattering medium of the leaf effectively increases the extinction coefficient by about two times and its variation (±14% S.D.) is mainly caused by light-scattering properties of the leaf.

© 2004 Elsevier B.V. All rights reserved.

Keywords: Leaf; Photosystem I; P700

1. Introduction

Two photosystems, PSII and PSI, operate sequentially in photosynthesis. Though absorbed photons are shared more or less equally between the photosystems [1,2], the area

densities of the reaction center complexes may vary [3]. For example, PSII density adjusts more flexibly to growth conditions than PSI density [4]. Still, data about the densities of the two photosystems are relatively scarce and frequently controversial because of difficulties of measurement. The density of active PSII can be conveniently measured as four times O₂ evolution from a saturating single-turnover flash in intact leaves [5,6], but there are no corresponding convenient methods for the measurement of PSI density.

Optical changes associated with shifts in redox states of chromophores can form the basis for measurement of e[−] carriers in photosynthesis. Distinct absorbance changes accompany reduction–oxidation of the donor pigment of PSI (P700), but in intact leaves optical measurements are

Abbreviations: Fd, ferredoxin; FeS, Rieske FeS complex; Chl, chlorophyll; Cyt *b*₆*f*, cytochrome *b*₆*f* complex; FRL, far red light; LHC, light-harvesting complex; PC, plastocyanin; PQ, plastoquinone; PSI, PSII, photosystem I and photosystem II; P700, PSI donor pigment; ST, single-turnover (flash); WL, white light

* Corresponding author. Department of Plant Physiology, Institute for Molecular and Cell Biology, Tartu University, 23 Riia St., Tartu 51010, Estonia. Tel.: +372 736 6021; fax: +372 742 0286.

E-mail address: alaisk@ut.ee (A. Laisk).

complicated. The absorbance change at 700 nm [7] is sensitive to overlapping dynamic Chl fluorescence and can be applied to optically thin chloroplast or thylakoid suspensions, but not to leaves [8]. The kinetic method based on the measurement of the speed of $P700^+$ reduction under the influence of a known e^- donation rate is suitable for use in intact leaves, but so far suffers from ambiguities caused by the complexity of the 810-nm signal [2].

In leaves the reduction–oxidation of P700 is observable as a change of transmittance (or reflectance) around 810 nm [9]. Chl does not absorb in this spectral region and modulated-light measurements prevent the possible interference by Chl fluorescence [10]. The reduced minus oxidized extinction coefficient of P700 for PSI particles is $8 \text{ mM}^{-1} \text{ cm}^{-1}$ at 815 nm [7], but this value cannot be used for intact leaves because of increased scattering [11]. Using the alpha band of Cyt *f* as a reference and assuming a 1:1 ratio between the densities of Cyt *f* and PSI, the extinction coefficient of $P700^+$ has been estimated to be about $115 \text{ mM}^{-1} \text{ cm}^{-1}$ in leaves [12]. It is conceivable that increased scattering of the beam in the leaf would increase the apparent extinction coefficient, but is the effect really so strong that the coefficient would increase by more than 10-fold?

In leaves the 810-nm absorbance change is complex, caused not only by $P700^+$, but also by PC^+ and reduced Fd [11]. Recently we proposed a method for deconvolution of the 810 nm signal, based on the oxidative titration of PSI donor side e^- carriers by FRL, which allows one to determine the component fractions of $P700^+$ and PC^+ in the total signal and to find the number of e^- in each of the partially reduced high-potential donor side carriers [13]. The oxidative titration method was based on the assumption that the PSI donor side carriers P700, PC and Cyt *f* are in redox equilibrium. In the present work, we applied a reductive titration method to confirm assumptions underlying the oxidative titration method. Single-turnover flashes of different quantum dose were applied to leaves in the presence of a FRL background illumination which selectively excites PSI. The number of e^- generated in PSII by a flash was measured as four times O_2 evolution. The corresponding differential 810–950-nm transmittance change was measured as these e^- reduced $P700^+$. Transmittance change caused by the reduction of $1 \text{ } \mu\text{mol m}^{-2}$ of $P700^+$ was calculated to find the effective differential extinction coefficient of $P700^+$ at 810–950 nm in leaves, which was $17.6 \pm 2.4 \text{ mM}^{-1} \text{ cm}^{-1}$. The result shows that the scattering medium of the leaf effectively increases the extinction coefficient by about two times.

2. Materials and methods

2.1. Plant material

Birch (*Betula pendula* Roth) leaves were sampled from a tree growing outdoors in spring 2003. In order to cover a

range of PSI densities, sun-exposed leaves were sampled during their development (beginning May 15, the leaves emerged at about 4–6 of May). Leaves of lilac (*Syringa vulgaris* L.), elm (*Ulmus glabra* L.) hawthorn (*Crataegus* sp.) and Bishop's weed (*Aegopodium podagraria* L.) were sampled in September. Excised leaves with their petioles in water were mounted in the leaf chamber of the gas exchange measurement system, where experiments lasted for about 2 h.

2.2. Gas exchange measurements

Properties of the two-channel fast-response measurement system (Fast-Est, Tartu, Estonia) have been described [2,13,14]. Part of a test leaf was enclosed in a sandwich-type chamber (diameter 31 mm, height 3 mm) and flushed with gas at a rate of 0.5 mmol s^{-1} . Leaf temperature was stabilized at 22°C and the water vapor pressure deficit of the flushing gas was maintained at 1.7 kPa. Desired O_2 and CO_2 concentrations in N_2 were generated by mixing pure cylinder gases at controlled flow rates. The CO_2 concentration was maintained at $360 \text{ } \mu\text{mol mol}^{-1}$ in all experiments. Most of the time O_2 concentration was $0.21 \text{ mol mol}^{-1}$, but was rapidly decreased to $50 \text{ } \mu\text{mol mol}^{-1}$ during the measurement of O_2 evolution pulses. The anaerobiosis did not last longer than 10 min. Oxygen evolution from the leaf was measured in the same flow-through system with a Zr-oxide O_2 analyzer Ametek S-3A (Thermox, Pittsburgh, PA).

2.3. Leaf illumination

The leaf chamber was illuminated through a multiarm plastic fiber-optic light guide (Fast-Est) from three sources which provided actinic WL, FRL (incident fluence rate $70 \text{ } \mu\text{mol quanta m}^{-2} \text{ s}^{-1}$, 720 nm narrow-band interference filter from Andover Corp. Salem, NH), and multiple turnover (10 ms) pulses of $11000 \text{ } \mu\text{mol quanta m}^{-2} \text{ s}^{-1}$. Computer-operated electro-pneumatic shutters (Fast-Est, full pulse edges of 1.3 ms) were used for synchronized control of the light sources. Single-turnover (ST) flashes of up to $60 \text{ } \mu\text{mol quanta m}^{-2}$, 4- μs length, were produced by a Machine Vision Strobe MVS-7060 (EG&G Optoelectronics, Salem, MA). Flashes were attenuated by neutral density filters when necessary and applied to the leaf through an arm of the light guide.

The absorption coefficients of the leaf for WL and for FRL were measured in an integrating sphere using a spectroradiometer PC-2000 (Ocean Optics, Dunedin, FL) calibrated against a standard lamp. The incident WL was measured by a LI-190SB quantum sensor (LiCor, Lincoln, NE). The spectral distribution of the WL and FRL was measured with the spectroradiometer PC-2000 and absorbed photon fluence rates of WL and FRL were computed from the spectral distributions of the light source and leaf absorbance [13].

2.4. Leaf transmittance measured differentially at 810 and 950 nm

A dual wavelength (810 and 950 nm) emitter-detector ED P700DW module together with a PAM 101 main control unit (H. Walz, Effeltrich, Germany) was used for the measurements in the transmittance mode. We shall refer to the output of this device as the ‘P700DW signal’. Primary measurements of transmittance change, caused by both P700⁺ and PC⁺, were deconvoluted to find the transmittance change per $\mu\text{mol P700}^+ \text{m}^{-2}$. The conventional spectrophotometric extinction coefficient ε ($\text{mM}^{-1} \text{cm}^{-1}$) was defined as:

$$\varepsilon = -10^4 \frac{\log(I/I_0)}{N_e} \quad (1)$$

where I/I_0 is the relative P700DW signal change and N_e is the corresponding $\mu\text{mol e}^- \text{m}^{-2}$ in P700 that generated the signal change. The numeric coefficient in the formula corrects for differences in units employed.

The system was operated and data were recorded using an A/D converter board ADIO 1600 (ICS Advent, San Diego, CA) and a system-operation and data-recording program RECO (Fast-Est).

3. Results

3.1. Experimental rationale

We generated e^- from water by exciting PSII (hereafter referred to as ‘PSII e^- ’) with ST flashes and measured the corresponding P700DW signal change when these e^- arrived at PSI. After pre-illumination to open stomata and attaining steady-state photosynthesis, WL was replaced by FRL that oxidized most, but not all, of the P700. The slow PSII excitation by FRL supported e^- flow of about $2 \mu\text{mol e}^- \text{m}^{-2} \text{s}^{-1}$ that randomized the s-states of the water-splitting complex [6], the two- e^- gate at the PSII acceptor side and the e^- transfer phases of the Q-cycle. The ambient O_2 concentration was decreased to about $50 \mu\text{mol mol}^{-1}$ and a ST flash was applied. The FRL beam was interrupted by a shutter simultaneously with the flash, immediately stopping e^- transport through PSI. The resulting transient in the P700DW signal was recorded over 1.5 s, following which FRL was turned on enabling averaging of transients over successive measurement periods of 10 s. The P700DW signal (Fig. 1A) showed an initial additional oxidation of P700 by the flash (time-resolved in Fig. 1B) followed by a fast phase of P700⁺ reduction caused by the PSII e^- arriving via Cyt b_6f . The transient in the P700 DW signal culminated in a slower phase reflecting reduction of interphotosystem carriers by e^- arriving from stromal reductants in the dark (we shall refer to these as ‘PSI e^- ’). The initial fast phase was absent when FRL was interrupted in the absence of a

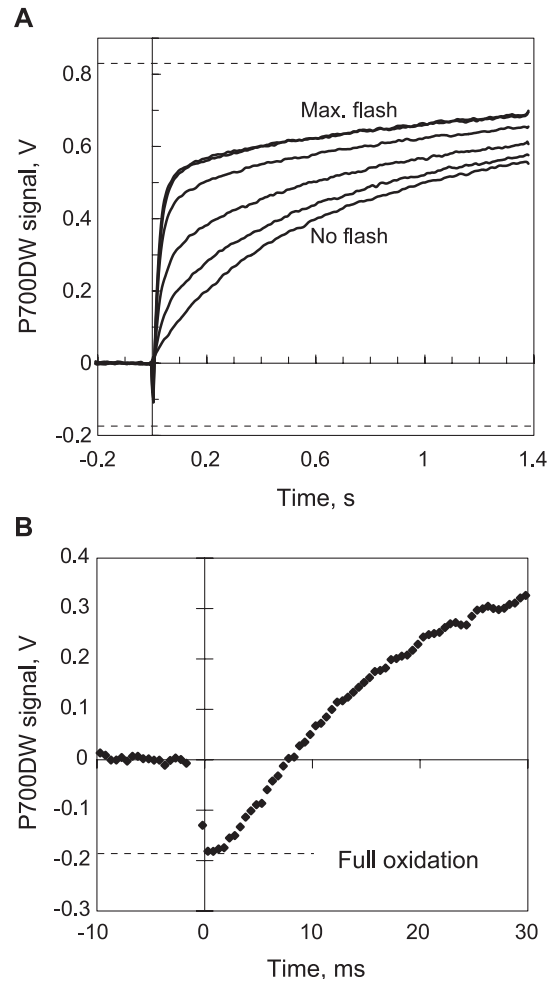


Fig. 1. Recorded traces of P700DW signal after ST flashes of different dose. Panel A: The leaf was pre-illuminated under FRL. At time zero, a ST flash was applied and FRL simultaneously interrupted. The uppermost curve was measured with maximum flash dose of $60 \mu\text{mol quanta m}^{-2}$, for other curves the flash was attenuated as shown in Fig. 4B and the lowest curve was recorded without a flash. The initial downward peak shows additional oxidation of P700, which increased with flash dose (resolved in Panel B for the maximum flash). Each trace is an average of three recordings (nine recordings in Panel B). Signal levels corresponding to full oxidation (bottom) and full reduction (top) of PSI donors are indicated by dotted lines. The minimum immediately after the maximum flash (dotted line in Panel B) was assumed to be the signal level corresponding to completely oxidized PC and P700.

flash because then donor side carriers were reduced only by the stromal reductants (PSI e^-). The maximum P700DW amplitude recorded following a saturating ST flash corresponded to full oxidation of P700 and other PSI donor side carriers. Quantitative interpretation of the fast phase caused by PSII e^- became possible after the P700DW signal traces of Fig. 1 were converted into the number of e^- in PSI donors.

3.2. P700DW signal conversion

The ST flashes were applied over a wide range of intensities. Owing to the different midpoint potentials of the

PSI donor side carriers, PSII e^- produced from weak flashes reduced mainly $P700^+$ while the saturating flashes reduced most of the $P700^+$, and part of the PC^+ , pools. Since the extinction coefficient of PC^+ is about 20% that of $P700^+$, the signal change per e^- was larger when $P700^+$ was the primary e^- acceptor, but it became smaller after $P700^+$ was almost completely reduced and PC^+ was the main e^- acceptor (higher signal amplitudes in Fig. 1). To consider this in calculations of the pools of e^- in P700 and PC, we applied a P700DW signal conversion algorithm, based on the oxidative titration of PSI donor side e^- carriers.

An oxidative titration, or ‘FRL titration’, curve is the time course of the P700DW signal during the oxidation of the PSI high-potential e^- donors (Rieske FeS, Cyt *f*, PC and P700) under FRL [13]. A leaf, pre-illuminated with FRL, was subjected to dark intervals of different length; after which the FRL was restored. The pre-oxidized PSI high-potential donors became reduced in the dark. The extent of reduction increased with length of the dark interval. The reoxidation trace in FRL was sigmoidal, beginning with a convex phase and ending with a concave exponential phase (Fig. 2). FeS+Cyt *f* and PC were oxidized during the initial convex phase, while P700 oxidation dominated during the exponential tail of the curve. As described previously [13], the initial convex phases of the oxidation traces measured after longer dark exposures could be horizontally shifted into coincidence, but the curves differed in their exponential phases wherein oxidation was slower after longer dark exposures. This shows that the quantum yield of PSI e^- transport was practically constant in the initial part of

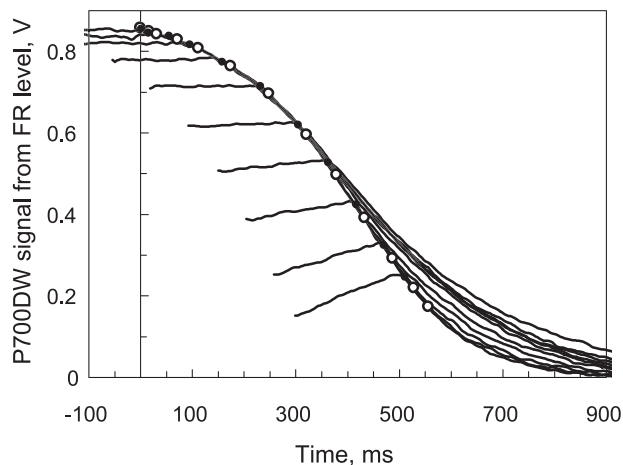


Fig. 2. Oxidative titration of the PSI high-potential donors with FRL. The leaf was exposed to FRL until a steady signal was attained. The FRL was then switched off for different time intervals. In the dark, electrons from stromal reductants reduced the high-potential donors to increasing extent with the length of the dark exposure (traces recorded during the last 200 ms of dark exposures are shown as the almost horizontal lines). After a dark exposure, the FRL was restored and the ensuing oxidation trace was recorded. Each curve was shifted into coincidence with the next curve of increased dark exposure at the denoted points (open circles). The resulting composite curve (lower boundary of the family, open circles) was fitted by a model that describes the process of oxidation of redox-equilibrated PSI donors [13].

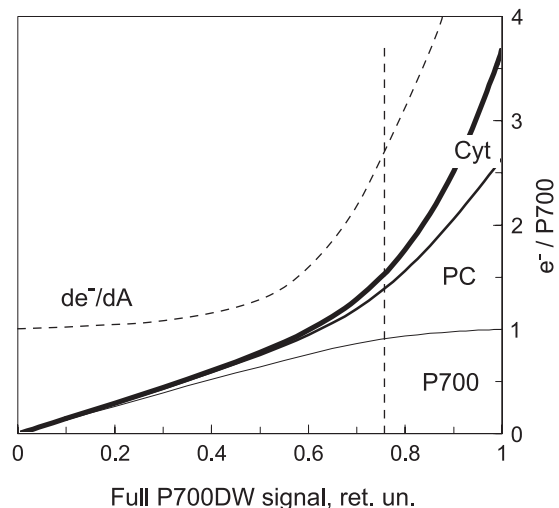


Fig. 3. An example of the deconvolution of the P700DW signal from the experiment of Fig. 2. The abscissa is P700DW signal relative to its full amplitude; 0 is complete oxidation, 1 is complete reduction. The heavy line shows the total number of e^- per P700 in the donor side carriers (maximum 3.7 in this example). Together the lines show the accumulation of e^- in P700, P700+PC, and P700+PC+(Cyt *f*+FeS). The derivative de^-/dA shows the increase in the number of e^- in the PSI donors per unit P700DW signal increase (same ordinate scale). The vertical dotted line indicates the signal caused by $P700^+$.

different curves, while Cyt *f* and PC were oxidized, but the yield tended to decrease at the end of the titration [13]. In order to ensure that the quantum yield was maximal, we used traces recorded after the shortest possible dark exposure to analyze the exponential phase. Thus, the oxidative titration curve selected for analysis by modeling was the lower boundary of the family of recorded traces in Fig. 2.

The P700DW signal transient during the FRL titration process was modeled on an assumption of redox equilibrium between the three e^- carrier pools, (Cyt *f*+Rieske FeS), PC and P700 [13]. The computed best fit to the measured titration curve yielded the sizes of (Cyt *f*+FeS), PC, and P700 and their standard redox potential (E_m) differences. Since the quantum yield of PSI e^- transport was so sensitive to the amount of previously transported e^- , we doubted that the highest observed quantum yield of PSI e^- transport was unity. By leaving the actual quantum yield of PSI under FRL as unknown, the model yielded relative (rather than absolute) pool sizes of e^- per P700 in PC and in (FeS+Cyt *f*) (Fig. 3). However, information obtained by this procedure was sufficient for the calculation of the % transmission change caused by the fully oxidized P700 (without PC^+). In order to calculate the apparent extinction coefficient of $P700^+$, this % transmission change was related to PSI density.

3.3. Determination of PSI density

The absolute PSI density was determined from the relative degree of $P700^+$ reduction caused by a known

density of PSII e^- , based, in turn, on O_2 evolution from the ST flash (Fig. 4A). The PSII e^- from low-dose flashes mainly reduced $P700^+$, while e^- from the more powerful flashes almost fully reduced $P700^+$ and partially reduced PC^+ , because typically PSII density exceeded PSI density. For each flash, the number of PSII e^- per P700 was calculated from the rapid-phase increase in the P700DW signal as the difference between converted time courses of e^- per P700 in traces with and without a flash (Fig. 5A). It was also necessary to account for e^- transported through PSI by the flash (the drop of the recorded line below the FRL level due to complete oxidation of P700, Fig. 1B). In Fig. 5B the pool of PSII electrons in $\mu\text{mol m}^{-2}$ measured from O_2 evolution is plotted versus the relative pool of e^- per PSI, calculated from the rapid phase of the P700DW signal (referenced to full oxidation of P700). The relationship is propor-

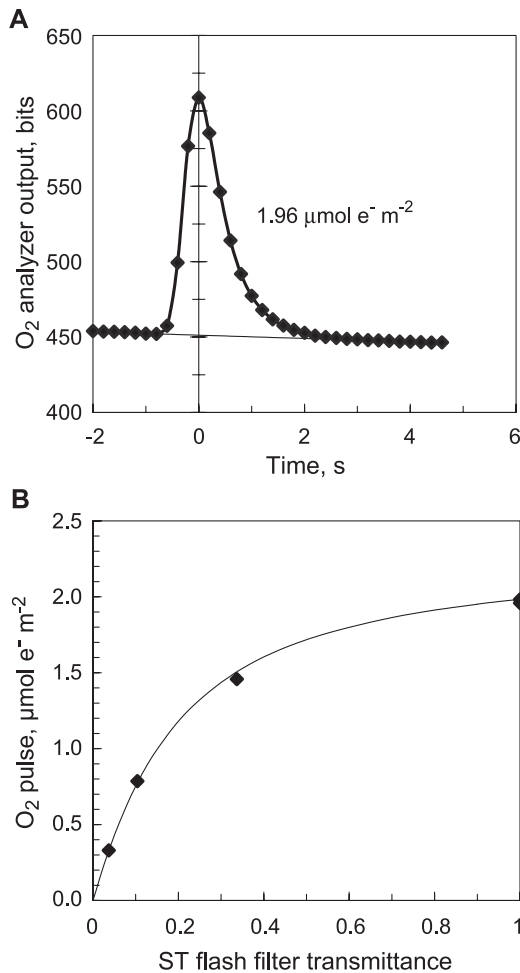


Fig. 4. A recorded trace of oxygen evolution after a full-dose ST flash (average of nine measurements, Panel A) and flash dose response of O_2 evolution (Panel B). The leaf was illuminated with FRL, O_2 concentration was decreased to $50 \mu\text{mol mol}^{-1}$, and the flash was applied. Traces from different flashes were integrated and the sum of $4 \times O_2$ evolution per flash was plotted against relative flash attenuation (dose of $60 \mu\text{mol quanta m}^{-2}$ corresponds to relative filter transmittance of 1).

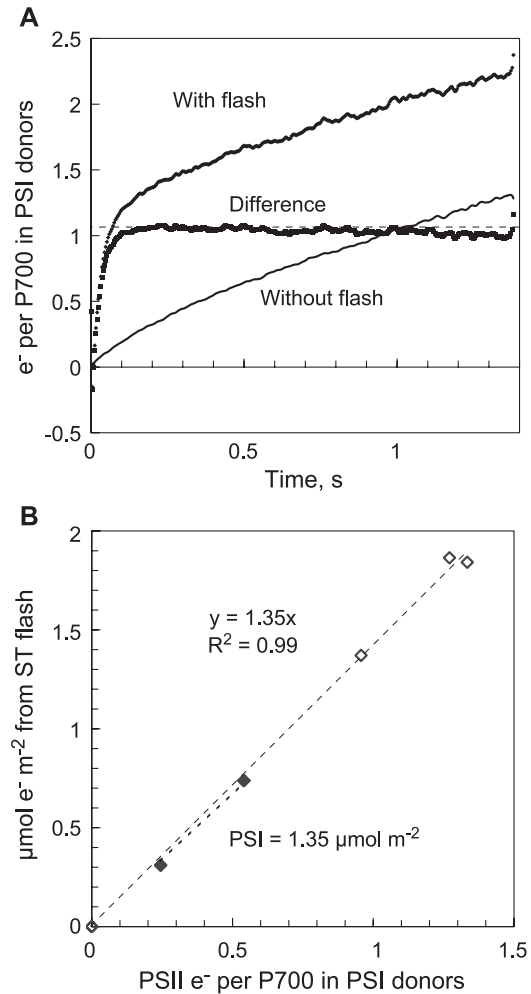


Fig. 5. Time courses of reduction of PSI donor side carriers with and without a ST flash and the difference due to the flash (Panel A, deconvoluted as shown in Fig. 3). Panel B compares the number of e^- generated by PSII during a ST flash (calculated from O_2 evolution) with electrons arriving at PSI (calculated from the rapid phase of the P700DW signal). Note that in Panel A, the $e^-/\text{P700}$ scale is arbitrarily set to 0 at the steady-state oxidation under FRL. The number of $e^-/\text{P700}$ due to oxidation by the flash is shown as a negative deflection. In Panel B, filled data points were mainly in the range of the $P700^+$ signal while open data points were in the range of the PC^+ signal. The slope of the regression line represents the density of PSI; here and in following figures, R^2 is correlation coefficient.

tional up to the maximum flash dose of $60 \mu\text{mol quanta m}^{-2}$. The slope of the line presents the absolute PSI density, which was $1.35 \mu\text{mol m}^{-2}$ in the given example. Since the maximum flash generated $1.8 \mu\text{mol } e^- \text{ m}^{-2}$, the PSII density exceeded the PSI density resulting in considerable reduction of PC^+ . We emphasize that our method involves independent assessments of O_2 evolution and change in P700DW signal caused by the ST flash. It is significant, therefore, that the relationship of Fig. 5B remained linear over a wide range of flash intensities, consistent with successful compensation by the P700DW signal conversion algorithm for contribution of PC^+ to the optical signal.

3.4. The effective extinction coefficient of P700⁺ in leaves

Having determined the partial optical signal generated by P700⁺ on one hand and the absolute PSI density on the other, we calculated the effective extinction coefficient of P700⁺ in the leaf as the ratio of these two quantities. Fig. 6 compares the partial optical signal from P700⁺ with the measured PSI density. The relationship is proportional, the reciprocal of the slope is 0.40% per $\mu\text{mol P700}^+ \text{ m}^{-2}$ with the correlation coefficient R^2 of 0.93 (S.D.=0.055 or $\pm 14\%$). For optical measurements in leaves, the appropriate presentation of the extinction coefficient is % transmittance change per $\mu\text{mol P700}^+ \text{ m}^{-2}$ as above. Converted into the common spectrophotometric units (Eq. (1), the extinction coefficient is 17.6 ± 2.4 (S.D.) $\text{mM}^{-1} \text{ cm}^{-1}$, measured differentially at wavelengths of 810 and 950 nm.

3.5. Oxidative titration of PSII electrons at PSI

To check whether all e^- generated in PSII arrived at PSI, we oxidatively titrated the number of e^- that arrived at PSI after a flash. The standard experimental arrangement was modified so that FRL was not interrupted simultaneously with application of the ST flash (Fig. 7). As a result, e^- arriving at PSI were transported to the acceptor side and P700 reduction proceeded through a maximum and returned to the steady-state level. We calculated the number of photons used to transport these e^- as the product of the known FRL quantum absorption rate times the integral of non-oxidized P700 during the transient. We considered as well that not only the flash-generated e^- , but also slow background e^- flow from the stroma, contributed to reduction of P700⁺. Hence, a reference line was constructed by modeling how the P700 reduction level

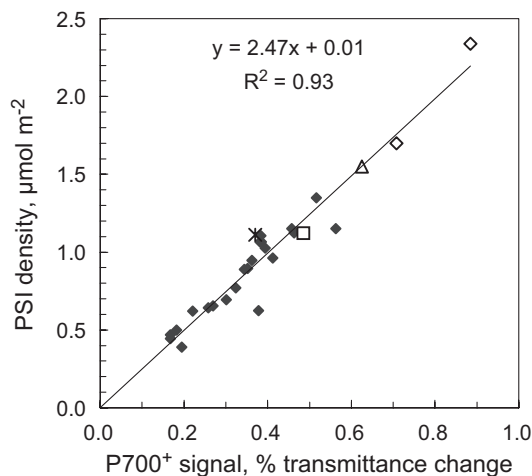


Fig. 6. Correlation between PSI density and the P700DW signal caused by P700⁺ in developing birch leaves (filled diamonds) and in fully-grown leaves of lilac (open square), elm (open diamond), hawthorn (open triangle) and Bishop's weed (asterisk).

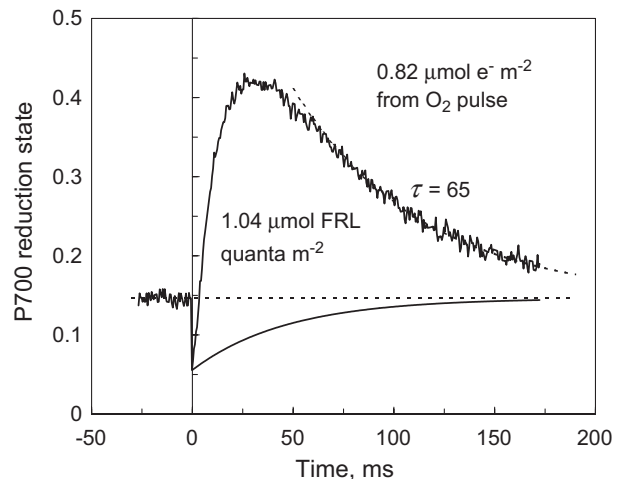


Fig. 7. Oxidative titration by FRL of the number of e^- that arrived at PSI after a ST flash. A ST flash was applied to a leaf, illuminated with FRL and, different from Fig. 1, FRL was not interrupted. The recorded P700DW signal transient was deconvoluted as the true time course of unoxidized P700. The reference line was constructed as explained in text and the number of FRL quanta used for transporting the PSII e^- was found by integration of the under-curve area.

would have changed if, subsequent to the initial oxidation by the flash, no e^- arrived at PSI from PSII. For this we used the time constant of the flashless reference curve of Fig. 1, which represents the speed of e^- arrival from stromal reductants.

In the experiment of Fig. 7, $0.82 \mu\text{mol e}^-$ were generated by the sub-saturating ST flash, as measured from O_2 evolution. The integration method described above indicated that $1.04 \mu\text{mol quanta m}^{-2}$ of FRL were used to transport these e^- through PSI. The excess of quanta consumed compared to the number of e^- transported is explainable in terms of a lower quantum yield of PSI e^- transport for the flash-generated e^- . We note that the time constant for the after-flash reoxidation of P700 ($\tau=65$ ms) is considerably longer than that for the fastest reoxidation time after the shortest dark exposure of Fig. 2 (40 ms). A progressive slowing of e^- transport through PSI was noticed previously and explained as the decrease in PSI quantum yield due to the accumulation of e^- in PSI acceptor side carriers [13]. Considering the latter, we find the agreement between e^- arrival in PSI based on O_2 evolution and FRL quantum consumption during transport of these e^- through PSI to be remarkably good. The results are inconsistent with considerable losses of e^- between PSII and PSI.

3.6. Correlative relationships

The complete procedure of reductive titration for determining PSI density was complex, requiring ST flashes and O_2 evolution measurements. Correlative relationships could enable routine approximation of PSI density from simpler optical parameters. Correlation between the full

P700DW signal amplitude (P700⁺ and PC⁺ together) and PSI density was only slightly weaker than the correlation between the P700⁺ signal and PSI density (0.90 instead of 0.93, Fig. 8A). This shows that the relative proportion of PC⁺ signal in the total was relatively constant and the ratio of the slopes of the regression lines $1.71/2.47=0.69$ indicates the average contribution of P700⁺ to the total P700DW signal.

The fact that FRL (720 nm) preferentially excites PSI is related to the presence of far-red-absorbing Chls in this reaction center. Assuming that the number of these Chls per reaction center is more or less constant, a proportional relationship is expected between the PSI density and leaf optical density at 720 nm. Indeed, this correlation (Fig. 8B) was as high as that of the P700⁺ component of the P700DW signal versus PSI density (both $R^2=0.93$). Correlation between total Chl and PSI density was also rather high, but it had an offset (Fig. 8C). In fully-grown leaves there were 340 Chl per PSI, and assuming that half of total Chl was attached to PSII, the PSI antenna size stabilized at 170 (210 in younger leaves) Chl per PSI. The correlation between PSI and PSII densities was relatively high in developing sun leaves of birch (Fig. 8D), but weak in fully developed leaves of other species. On average, in developing birch leaves PSII density was 1.24 times the PSI density.

4. Discussion

4.1. Using the 810-nm transmission signal for the analysis of PSI in leaves

The oxidized forms of the two high-potential e⁻ carriers P700⁺ and PC⁺ have a wide absorbance maximum around 810 nm, which is easy to measure. Facilitated by the commercially available equipment [10,14], a number of papers have appeared wherein e⁻ transport through PSI has been analyzed using this signal. A major problem with these measurements is that the reduction–oxidation difference spectra of P700/P700⁺ and PC/PC⁺ overlap and the apparent extinction coefficients of the two compounds in the scattering medium of intact leaves are not known. In most work, the total 810-nm signal has been assumed to be more or less proportional to the P700⁺ signal [15]. The approach is based on a report that in a dynamic situation of fast photosynthesis the apparent equilibrium constant between P700 and PC may approach unity [16] so that the oxidation states of the two e⁻ carriers change in parallel [1,17]. Recently, an algorithm was proposed that deconvolutes the total 810-nm signal into P700⁺ and PC⁺ components [13]. The procedure is based on mathematical modeling of the time course of the oxidation of the PSI donor side under FRL—so-called “oxidative titration” or

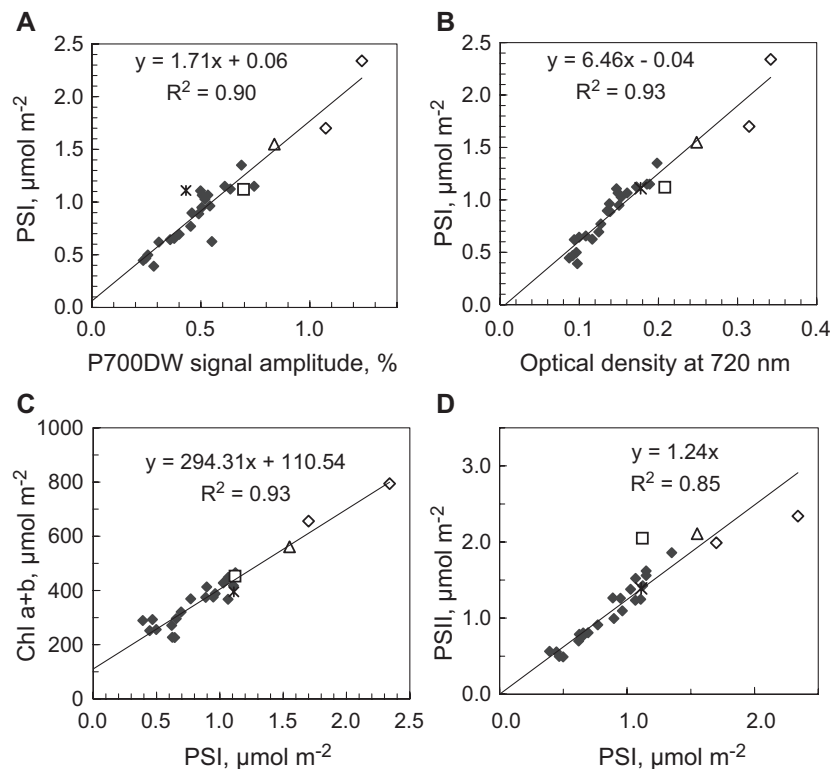


Fig. 8. Correlation between PSI density and optical parameters of the leaf in developing birch leaves (filled diamonds), fully-grown leaves of lilac (open square), elm (open diamond), hawthorn (open triangle) and Bishop's weed (asterisk). Panel A: correlation with the full P700DW signal amplitude; Panel B: correlation with leaf optical density at 720 nm; Panel C: correlation with total chlorophyll content; Panel D: correlation between PSI and PSII densities.

“FRL titration” curves. The model assumes equilibrium among the three PSI donor side carriers P700, PC, and Cyt *f* (+Rieske FeS). The best fit was obtained at a ΔE_m of 80 mV between P700 and PC, indicating a strong non-proportionality between the total and P700⁺ signals. In this work we applied the deconvolution algorithm to analyze the change in optical signal generated by arrival of a known number of e[−] to the PSI donor side. The e[−] were generated by a ST flash and their number was measured from the accompanying O₂ evolution pulse (e[−] m^{−2}). The optical signal change measured with the dual wavelength sensor P700DW reflected, on a relative scale, how many e[−] per P700 arrived at the PSI donor side. The strict proportionality between these two quantities, one measured from O₂ evolution and the other calculated from the P700DW signal (Fig. 5B, $R^2=0.995$), is consistent with successful deconvolution of P700⁺ and PC⁺ signals by the P700DW signal conversion algorithm based on the oxidative (FRL) titration technique [13]. The result also shows that the slow e[−] transport that occurs under FRL cannot shift the PSI donor side carriers out of equilibrium, supporting the theory of equilibrium between the PSI donor side carriers [18]. This methodological breakthrough enables calculation of the number of e[−] in the PSI donor side carriers as well as the amplitude of the partial signal that is corresponding to the reduction–oxidation difference of P700. By relating the latter to PSI density, we determined the effective extinction coefficient of P700⁺ in the scattering medium of leaves.

4.2. The effective extinction coefficient of P700⁺

The average value of the effective extinction coefficient for P700⁺, $0.40 \pm 0.055\%$ (0.67 \AA^2 of optical cross-section area per molecule) or $\epsilon=17.6 \text{ mM}^{-1} \text{ cm}^{-1}$, found in this work is greater than the value of $8 \text{ mM}^{-1} \text{ cm}^{-1}$ reported for PSI particles [7]. The difference is expected considering the increased scattering of radiation in leaves, but the value is still much smaller than $115 \text{ mM}^{-1} \text{ cm}^{-1}$ estimated from comparison with the extinction coefficient of Cyt *f* in leaves [12]. Since we used a modified detector, the extinction coefficient was determined for the wavelength difference 810–950 nm. Considering the P700⁺–PC⁺ spectrum for chloroplasts (Fig. 8 of Ref. [11]) the single-wavelength value for 810 nm may be about 20–25% greater than for the 810–950 nm difference, but would be about the same for the standard 810–900-nm dual wavelength ED P700DW.

A number of factors such as scattering-induced enhancement of absorption and flattening of bands affect the extinction coefficient in intact leaves [11,19,20]. Considering the possible experimental error of O₂ evolution measurements ($\pm 1\%$ for saturating flashes and $\pm 5\%$ at low flash doses) and of the segregation of the signals from PSII e[−] and from PSI e[−], we estimated that a big part of the variation of the results ($\pm 14\%$ S.D.) was caused by variations in leaf structure. In some leaves ϵ could be 50%

greater than the average. Thus, although random experimental error certainly contributed to variation in the extinction coefficient for P700, differences in structure among developing leaves and leaves of different species used in our experiments introduced another source of variability.

Values of ϵ could be systematically biased, e.g. overestimated, if the O₂ evolution measurements were underestimated due to reassimilation of O₂. During the measurements O₂ concentration in the leaf chamber was between 50 and 100 $\mu\text{mol mol}^{-1}$, under which mitochondrial respiration was clearly O₂-limited and reassimilation of photosynthetic O₂ in mitochondria was possible. We detected a significant decrease in the O₂ evolution pulses when stomatal conductance was very low, but the relationship leveled off at moderate and greater stomatal conductances typical of those observed in these experiments (data not shown). Thus, it is unlikely that the reassimilation of O₂ caused a significant systematic overestimation of ϵ .

An important question relates to how accurately O₂ evolution reports e[−] transfer from PSII to PSI during a ST flash. Known aspects of the relevant e[−] transport mechanisms permit alternative stoichiometries of O₂ evolution, PSII charge separation, and reduction of P700⁺ under non-steady-state versus steady-state conditions. If a ST flash is applied after prolonged darkness O₂ is not evolved because the *s*₄ state in PSII is not present. Furthermore, e[−] flow from PSII to PSI could be impeded since the secondary acceptor Q_B cannot become doubly reduced in most PSII complexes and e[−] transfer by the Q-cycle is equally divided between Cyt *f* and Cyt *b*. In our experiments background illumination with FRL excited not only PSI, but also PSII, resulting in a slow linear e[−] transport rate of 1 to 2 $\mu\text{mol e}^{-} \text{ m}^{-2} \text{ s}^{-1}$. Our analysis of the excursion in P700 redox state in relation to O₂ production following a superimposing ST flash (Fig. 7) did not indicate a violation of the one-to-one stoichiometry of charge separation in PSII and PSI during e[−] transport from H₂O to CO₂. We conclude that the background FRL randomized all e[−] gates so that the ratio of O₂ evolved to e[−] arriving at PSI during the ST flash was identical to that occurring during steady-state photosynthesis.

In the reductive titration method, a major interfering factor was the spontaneous e[−] arrival from stromal reductants in the dark (termed PSI e[−] flow). Normally, this rate is much slower than e[−] donation from PSII via Cyt *b*₆*f* and sometimes it is interpreted as cyclic e[−] transport [21]. In our experiments, the flows of PSII e[−] and PSI e[−] were not readily distinguishable by their time kinetics, because the rate of PSII e[−] flow was relatively slow. Typically, the time of e[−] transfer through Cyt *b*₆*f* is about 6 ms or less [2,22] but it may increase to 30–40 ms in the presence of strong photosynthetic control exerted by transthylakoid pH gradient [23]. In our experiments under continuous FRL photosynthetic control was minimal, but the relatively slow establishment of the signal from PSII electrons (time constant about 30 ms, Fig. 5A) evidently was caused by

the very low concentration of reduced PQ—only one reduced PQ per several PSII. Additional time could be introduced by PC cross-diffusion between PSI complexes if two e^- happened to arrive at one PSI in sequence [24]. Also, transfer of e^- through Cyt b_6f could be slowed by the organization of PQ into microdomains [25]. These processes together increased the e^- transport time between the photosystems by about fivefold, compared with the basic e^- transport time for a highly reduced PQ pool. Despite this, deconvolution of the measurements with and without flashes in the number of e^- per P700 successfully distinguished the signal caused by PSII e^- (Fig. 5A).

4.3. Correlative relationships

As expected, the apparent extinction coefficient of $P700^+$ in leaves was not constant, but varied, evidently dependent on scattering of the measurement beam in the leaf structure. Still, for the practical use of the ED P700DW instrument in ecophysiology, quantification of the $P700^+$ signal in terms of PSI density with S.D. of $\pm 14\%$ may be adequate. Moreover, the relationship between the full P700DW signals ($P700^+$ and PC^+ signals together) was strongly proportional to PSI density ($R^2=0.90$). The ratio of the slopes of the regression lines in Figs. 6 and 8A ($1.71/2.47=0.69$) shows that, on average, $P700^+$ accounted for 69% of the total signal; the remainder was due to PC^+ . In single-beam instruments the PC^+ portion of the signal has been estimated to be about 35% [10] or 40–50% [26]. The dual-beam instrument P700DW has a smaller PC^+ signal, in accordance with Ref. [11] and our earlier report [13]. The average $PC/P700$ ratio was 1.86 in our leaves, which agrees well with a prior report [27]. We emphasize that the correlation of Fig. 8A is between PSI density and the full P700DW signal amplitude, obtained by applying a saturation pulse on top of FRL. The deflection under FRL is 10–20% smaller than the full amplitude; it depends on FRL intensity, its quantum efficiency and on the e^- flux from the stromal reductants, so that the deflection under FRL alone cannot be recommended for estimation of PSI density in leaves.

The high correlation between the leaf optical density at 720 nm and the PSI density ($R^2=0.93$, Fig. 8B) shows that the number of far-red Chls (“red Chls” of Ref. [28]) per PSI was relatively constant in our leaves. Since the far-red Chls are embedded in PSI core proteins, as well as in LHCI [28], the correlation of Fig. 8C shows that the number of far-red Chls stabilized relatively early in PSI complexes of young leaves.

The correlation between PSI and PSII densities was good in developing birch leaves, about 1.24 PSII per PSI, but the proportionality across fully-grown leaves of different species was poor (Fig. 8D). This result is consistent with one series of reports [4,29], but in other experiments PSII and PSI densities were about equal [29] or PSII density was even smaller than PSI density [30]. Our data confirm that

there is generally no fixed stoichiometry with respect to PSII and PSI densities [31], though the PSII/PSI ratio may be subject to tighter control during development under sun-exposed conditions, as evidenced by the birch leaves of our experiments.

Acknowledgements

This work was supported by a personal Research Professorship grant to A.L. from Estonian Academy of Science and by Grant 5236 from Estonian Science Foundation. We express our gratitude to Dr. Richard B. Peterson for a critical reading of the manuscript.

References

- [1] H. Eichmann, A. Laisk, Cooperation of photosystems II and I in leaves as analysed by simultaneous measurements of chlorophyll fluorescence and transmittance at 800 nm., *Plant Cell Physiol.* 41 (2000) 138–147.
- [2] A. Laisk, V. Oja, B. Rasulov, H. R  mma, H. Eichmann, I. Kasparova, H. Pettai, E. Padu, E. Vapaavuori, A computer-operated routine of gas exchange and optical measurements to diagnose photosynthetic apparatus in leaves, *Plant Cell Environ.* 25 (2002) 923–943.
- [3] A. Melis, Spectroscopic methods in photosynthesis: photosystem stoichiometry and chlorophyll antenna size, *Philos. Trans. R. Soc. Lond., B* 323 (1989) 397–409.
- [4] W.S. Chow, J.M. Anderson, A.B. Hope, Variable stoichiometries of photosystem 2 to photosystem 1 reaction centres, *Photosynth. Res.* 17 (1988) 277–281.
- [5] W.S. Chow, A.B. Hope, J.M. Anderson, Oxygen per flash from leaf disks quantifies photosystem 2, *Biochim. Biophys. Acta* 973 (1989) 105–108.
- [6] V. Oja, A. Laisk, Oxygen yield from single turnover flashes in leaves: non-photochemical excitation quenching and the number of active PSII, *Biochim. Biophys. Acta* 1460 (2000) 291–301.
- [7] T. Hiyaama, B. Ke, Difference spectra and extinction coefficients of $P700$, *Biochim. Biophys. Acta* 267 (1972) 160–171.
- [8] W. Haehnel, V. Hesse, A. Pr  pper, Electron transfer from plastocyanin to $P700$. Function of a subunit of photosystem I reaction centre, *FEBS Lett.* 111 (1980) 79–82.
- [9] J. Harbinson, F.I. Woodward, The use of light-induced absorbance changes at 820 nm to monitor the oxidation state of P-700 in leaves, *Plant Cell Environ.* 10 (1987) 131–140.
- [10] U. Schreiber, C. Klughammer, C. Neubauer, Measuring P700 absorbance changes around 830 nm with a new type pulse modulation system, *Z. Naturforsch.* 43c (1988) 686–698.
- [11] C. Klughammer, U. Schreiber, Analysis of light-induced absorbance changes in the near-infrared spectral region: I. Characterization of various components in isolated chloroplasts, *Z. Naturforsch.* 46c (1991) 233–244.
- [12] C.A. Sacksteder, D.M. Kramer, Dark-interval relaxation kinetics (DIRK) of absorbance changes as a quantitative probe of steady-state electron transfer, *Photosynth. Res.* 66 (2000) 145–158.
- [13] V. Oja, H. Eichmann, R.B. Peterson, B. Rasulov, A. Laisk, Deciphering the 820 nm signal: redox state of donor side and quantum yield of photosystem I in leaves, *Photosynth. Res.* 78 (2003) 1–15.
- [14] C. Klughammer, U. Schreiber, Measuring P700 absorbance changes in the near infrared spectral region with a dual wavelength pulse

- modulation system, in: G. Garab (Ed.), *Photosynthesis: Mechanisms and Effects*, vol. 5, Kluwer Academic Publishers, Dordrecht, The Netherlands, 1998, pp. 4357–4360.
- [15] P.H. van Vliet, J. Harbinson, Modelling steady state P700 photo-oxidation in leaves: the role of plastocyanin, *Research in Photosynthesis*, vol. II, Kluwer Acad. Publ., Dordrecht, 1992, pp. 7.527–7.529.
- [16] P. Joliot, A. Joliot, Electron transfer between the two photosystems. Equilibrium constants, *Biochim. Biophys. Acta* 765 (1984) 219–226.
- [17] B. Genty, J. Harbinson, Regulation of light utilization in photosynthetic electron transport, in: N.R. Baker (Ed.), *Photosynthesis and the Environment*, Kluwer Acad. Publ., The Netherlands, 1996, pp. 67–99.
- [18] F. Drepper, M. Hippler, W. Nitschke, W. Haehnel, Binding dynamics and electron transfer between plastocyanin and photosystem I, *Biochemistry* 35 (1996) 1282–1295.
- [19] P. Latimer, C.A.H. Eubanks, Absorption spectroscopy of turbid suspensions: a method of correcting for large systematic distortions, *Arch. Biochem. Biophys.* 98 (1962) 274–285.
- [20] D.M. Kramer, A.R. Crofts, Control and measurement of photosynthetic electron transport, in: N.R. Baker (Ed.), *Photosynthesis and the Environment*, Kluwer Acad. Publ., The Netherlands, 1996, pp. 25–66.
- [21] N. Bukhov, E. Egorova, R. Carpentier, Electron flow to photosystem I from stromal reductants in vivo: the size of the pool of stromal reductants controls the rate of electron donation to both rapidly and slowly reducing photosystem I units, *Planta* 215 (2002) 812–820.
- [22] U. Siggel, The control of electron transport by two pH-sensitive sites, in: M. Avron (Ed.), *Proc. 3rd Internat. Congr. on Photosynth.*, Elsevier, Amsterdam, 1974, pp. 645–654.
- [23] A. Laisk, V. Oja, Range of the photosynthetic control of postillumination P700 reduction rate in sunflower leaves, *Photosynth. Res.* 39 (1994) 39–50.
- [24] M. Spittel, S. Andree, H. Kirchhoff, E. Weis, Control of linear electron flow by redistribution of cyt b_6/f from grana to stroma lamellae in 'state 2', in: P. Mathis (Ed.), *Photosynthesis: From Light to Biosphere*, vol. III, Kluwer Academic Publishers, Dordrecht, 1995, pp. 241–244.
- [25] H. Kirchhoff, S. Horstmann, E. Weis, Control of the photosynthetic electron transport by PQ diffusion microdomains in thylakoids of higher plants, *Biochim. Biophys. Acta* 1459 (2000) 148–168.
- [26] G. Schansker, A. Srivastava, Govindjee, R.J. Strasser, Characterization of the 820-nm transmission signal paralleling the chlorophyll a fluorescence rise (OJIP) in pea leaves, *Funct. Plant Biol.* 30 (2003) 785–796.
- [27] T. Graan, D.R. Ort, Quantitation of the rapid electron donors to P700, the functional plastoquinone pool, and the ratio of the photosystems in spinach chloroplasts, *J. Biol. Chem.* 259 (1984) 14003–14010.
- [28] B. Gobets, R. van Grondelle, Energy transfer and trapping in photosystem I, *Biochim. Biophys. Acta* 1507 (2001) 80–99.
- [29] K.O. Burkey, Effect of growth irradiance on plastocyanin levels in barley, *Photosynth. Res.* 36 (1993) 103–110.
- [30] W.-J. Lee, J. Whitmarsh, Photosynthetic apparatus of pea thylakoid membranes, *Plant Physiol.* 89 (1989) 932–940.
- [31] W.S. Chow, A.B. Hope, The stoichiometries of supramolecular complexes in thylakoid membranes from spinach chloroplasts, *Aust. J. Plant Physiol.* 14 (1987) 21–28.